Check for updates

Lifespan normative data on rates of brain volume changes

Marco Battaglini [a], Giordano Gentile [a], Ludovico Luchetti [a], Antonio Giorgio [a], Hugo Vrenken [b], Frederik Barkhof [b,c,d], Keith S. Cover [b,e], Rohit Bakshi [f], Renxin Chu [f], Maria Pia Sormani [g], Christian Enzinger [h,i], Stefan Ropele [h], Olga Ciccarelli [j,d], Claudia Wheeler-Kingshott [j,k,l], Marios Yiannakas [j], Massimo Filippi [m], Maria Assunta Rocca [m], Paolo Preziosa [m], Antonio Gallo [n], Alvino Bisecco [n], Jacqueline Palace [o], Yazhuo Kong [p,q], Dana Horakova [r], Manuela Vaneckova [s], Claudio Gasperini [t], Serena Ruggieri [t], Nicola De Stefano [a,*], on behalf of the MAGNIMS Study Group

[a] Department of Medicine, Surgery and Neuroscience, University of Siena, Siena, Italy
[b] Department of Radiology and Nuclear Medicine, MS Center Amsterdam, Amsterdam, the Netherlands
[c] Institutes of Neurology and Healthcare Engineering, UCL London, UK
[d] National Institute for Health Research (NIHR), University College London Hospitals (UCLH) Biomedical Research Centre (BRC), London, UK
[e] Department of Physics and Medical Technology, VU University Medical Center, Amsterdam, the Netherlands
[f] Laboratory for Neuroimaging Research, Ann Romney Center for Neurologic Diseases, Brigham and Women's Hospital, Harvard Medical School, Boston, MA, USA
[g] Department of Health Sciences (DISSAL), University of Genoa, Genoa, Italy
[h] Department of Neurology, Medical University of Graz, Graz, Austria
[i] Division of Neuroradiology, Vascular & Interventional Radiology, Department of Radiology, Medical University of Graz, Graz, Austria
[j] Queen Square Multiple Sclerosis Centre, UCL Institute of Neurology, University College, London, UK
[k] Brain MRI 3T, UK Research Center, C. Mondino National Neurological Institute, Pavia, Italy
[l] Department of Brain and Behavioural Sciences, University of Pavia, Pavia, Italy
[m] Neuroimaging Research Unit, Institute of Experimental Neurology, Division of Neuroscience, San Raffaele Scientific Institute, Vita-Salute San Raffaele University, Milan, Italy
[n] Department of Medical, Surgical, Neurological, Metabolic and Aging Sciences, University of Campania Luigi Vanvitelli, Naples, Italy
[o] Nuffield Department of Clinical Neurosciences, Oxford University Hospitals NHS Trust, University of Oxford, Oxford, UK
[p] CAS Key Laboratory of Behavioral Science, Institute of Psychology, Beijing, China
[q] Department of Psychology, University of Chinese Academy of Sciences, Beijing, China
[r] Department of Neurology and Center of Clinical Neuroscience, First Faculty of Medicine, Charles University and General University Hospital in Prague, Prague, Czech Republic
[s] Department of Radiodiagnostics, First Faculty of Medicine Charles University and General University Hospital in Prague, Prague, Czech Republic
[t] Department of Neurosciences S Camillo Forlanini Hospital, Rome, Italy

ARTICLE INFO

ABSTRACT

We provide here normative values of yearly percentage brain volume change (PBVC/y) as obtained with Structural Imaging Evaluation, using Normalization, of Atrophy, a widely used open-source software, developing a PBVC/y calculator for assessing the deviation from the expected PBVC/y in patients with neurological disorders. We assessed multicenter (34 centers, 11 acquisition protocols) magnetic resonance imaging data of 720 healthy participants covering the whole adult lifespan (16 −90 years). Data of 421 participants with a follow-up > 6 months were used to obtain the normative values for PBVC/y and data of 392 participants with a follow-up <1 month were selected to assess the intrasubject variability of the brain volume measurement. A mixed model evaluated PBVC/y dependence on age, sex, and magnetic resonance imaging parameters (scan vendor and magnetic field strength). PBVC/y was associated with age ($p < 0.001$), with 60- to 70-year-old participants showing twice more volume decrease than participants aged 30−40 years. PBVC/y was also associated with magnetic field strength, with higher decreases when measured by 1.5T than 3T scanners ($p < 0.001$). The variability of PBVC/y normative percentiles was narrower as the interscan interval was longer (e.g., 80th normative percentile was 50% smaller for participants with 2-year than with

1-year follow-up). The use of these normative data, eased by the freely available calculator, might help in better discriminating pathological from physiological conditions in the clinical setting.

1. Introduction

Neurodegenerative disorders are characterized by clinically relevant, irreversible brain tissue loss (i.e., atrophy) that begins at early stages and progresses relentlessly throughout the course of the disease (Frisoni et al., 2010; Rocca et al., 2017). Measures of brain volume changes as derived by magnetic resonance imaging (MRI) have been used in these disorders as index of neuro-degeneration (De Stefano et al., 2014; Hotter et al., 2009; van Maurik et al., 2017). Because halting neurodegeneration and promoting neuroprotection are the main targets of current therapeutic strategies in neurodegenerative diseases, these measures have been extensively applied in the context of both research studies and clinical trials (Giorgio and De Stefano, 2013).

Over the last 2 decades, substantial effort has been spent in improving MRI-derived methods of brain volume (BV) measurement. This has led to significant technical advancements, with several automated software tools that have shown ability in measuring BV loss with sensitivity, reproducibility, accuracy, and precision (Vrenken et al., 2013). However, because of a number of constraints, at present the assessment of BV loss is not routinely performed in clinical practice (De Stefano et al., 2017; Rocca et al., 2017; Sastre-Garriga et al., 2017). In this context, the lack of normative data does not allow the quantification of the variability due to different acquisition protocols and scanner types in BV measurement, and therefore, the use of these measurements becomes particularly challenging in the clinical setting. Indeed, normative data of MRI-derived measures of BV are important as they (1) may clarify the impact of important technical issues on the BV measures and (2) may be relevant in assessing deviations from normal behavior, as expected for age, sex, and MRI acquisition settings, both at group and individual levels.

Some studies have assessed MRI-derived BV changes in healthy individuals (Driscoll et al., 2009; Fotenos et al., 2005; Liu et al., 2003; Marcus et al., 2010; Opfer et al., 2017; Takao et al., 2012). Most of them, however, have investigated BV changes on populations with limited age span (i.e., older adult) (Fotenos et al., 2005; Liu et al., 2003). Even when performed over a broader range of adulthood, they had small sample sizes or were center specific (i.e., using single MR scanner and acquisition protocol) (De Stefano et al., 2016; Opfer et al., 2017; Takao et al., 2012). Overall, these studies seem to suggest that the rate of atrophy increases with age and that there are no significant sex-related differences in atrophy rates (Liu et al., 2003; Takao et al., 2012). By and large, the most comprehensive description of the rate of BV loss occurring in healthy individuals over the lifespan probably comes from a recent meta-analysis of 56 different longitudinal studies (Hedman et al., 2012). However, because of its design (i.e., analysis of aggregate statistics from each longitudinal study), this study was also unable to provide answers on the role of different MRI acquisition protocols and settings, thus limiting the clinical utility of the resulting rates of BV changes. A large longitudinal study assessing individual data processed in a standard fashion is therefore still lacking.

Against this background, the present study aimed to assess, in a relatively large population of healthy individuals covering the whole adult lifespan, longitudinal BV changes from MRI data acquired in multiple centers. The size of the analyzed population allowed addressing issues such as the relevance of sex and age on BV changes with higher statistical power than in the past. The primary goal was to provide normative values of yearly percentage brain volume change (PBVC/y) as obtained with Structural Imaging Evaluation, using Normalization, of Atrophy (SIENA) (Smith et al., 2002), which is a widely used open-source software. The presence of a large, multicenter scan-rescan MRI data set of healthy individuals with variable follow-up length allowed the MR-related sources of variability (e.g., different vendors, magnetic field strengths, acquisition parameters, and within-patient BV fluctuations) to be estimated and these were all taken into account in the statistical model that provides normative values of the rates of BV change.

2. Materials and methods

2.1. Participants

This is a multicenter, retrospective study based on the analysis of longitudinal MR data sets of healthy individuals. A total of 3077 anonymized conventional 3D T1-weighted (T1-W) images of 720 healthy individuals were collected from (Table 1) (1) data of 8 European imaging centers of the MAGNIMS (Magnetic Resonance Imaging in MS; www.magnims.eu) network, (2) data of the Laboratory for Neuroimaging Research, Harvard Medical School, Boston, MA, (3) data of the Department of Radiodiagnostics, Charles University, Prague, Czech Republic, and (4) a selected data set of the ADNI (Alzheimer's Disease Neuroimaging Initiative; www.loni.usc.edu/ADNI) network, mainly older participants scanned on 1.5 Tesla (T) GE scanners. Details on demographics and MRI characteristics of the healthy population in each participating center are reported in Table 1. Out of the 720 healthy individuals, a subset of 421 participants with a follow-up > 6 months was used to obtain the normative values for PBVC/y (Table 2) and a subset of 392 participants with a follow-up <1 month was selected to assess the intrasubject variability of the BV measurement using the SIENA software in different acquisition settings (Table 3). At each center, participants were included if they had no history of neurological or psychiatric disorders and if all T1-W images were acquired with the same procedure/sequence and scanner. For each data set, MRI scans were acquired after consent obtained from each participant in each center. The final study protocol was reviewed and approved by the European MAGNIMS collaboration for the analysis of pseudo-anonymized scans.

2.2. MRI acquisition

Data are summarized in Table 1. MRI data sets came from 10 academic centers (n = 622) and the ADNI database (n = 98 from 24 sites with identical acquisition protocol) and were acquired on scanners at both 1.5 and 3T from the three leading vendors (i.e., Siemens Healthcare, Philips Medical Systems, and GE Healthcare). There were no limits on the between-scan interval and on the number of scans for each participant. For each participant, data were acquired with the same scanner and acquisition protocol for the whole follow-up period. None of the scanners were changed or underwent major upgrades during the study period. Each data set was sent to the Quantitative Neuroimaging Laboratory of the University of Siena for quality control and centralized analysis.

Table 1
Demographics of the healthy individuals and MRI acquisition characteristics of each participating center

Center	No. of participants (male)	Mean age (SD)	Magnetic field strength and vendor	Slice thickness (mm)	Acquisition plane	T1 sequence types	Head coil channels	Distortion correction
ADNI	96 (48)	76.3 (4.6)	1.5 T GE	1.2	Axial	MPRAGE	8 channels	Yes
Amsterdam	56 (24)	43.1 (9.8)	1.5 T Siemens	1.3	Coronal	MPRAGE	8 channels	No
Boston	51 (17)	38.7 (9.2)	1.5 T GE	1.2	Sagittal	3D-SPGR	4 channels	Yes
			3T GE	1.6	Coronal	3D-MTEFT	8 channels	
			3T Siemens	1	Sagittal	3D-MPRAGE	20 channels	
Graz	155 (80)	29.7 (16)	3T Siemens	1	Sagittal	MPRAGE	12 channels	No
London	87 (43)	36.7 (11.1)	3T Philips	1	Sagittal	3D-TFE	32 channels	Yes
Milan	157 (76)	27.2 (10.8)	3T Philips	0.8	Axial	3D, short TR spoiled, gradient echo	8 channels	Yes
Naples	26 (15)	41 (9.9)	3T GE	1.2	Sagittal	3D, T1 magnetization prepared fast spoiled gradient echo	8 channels	No
Oxford	15 (4)	50 (15.9)	3T Siemens	1	Axial	MPRAGE	32 channels	No
Prague	83 (38)	35.5 (10)	1.5 T Philips	1	Axial	3D T1 FFE	8 channels	No
Rome	13 (7)	36.5 (10.5)	1.5 T Siemens	1	Axial	3D T1 gradient echo	6 channels	No
Siena	37 (17)	37.4 (10.2)	1.5 T Philips	3	Axial	Gradient echo	8 channels	No
Total	720							

Key: ADNI, Alzheimer's Disease Neuroimaging Initiative; MRI, magnetic resonance imaging.

2.3. MRI data analysis

2.3.1. Image preprocessing

An initial quality control was visually performed by expert neuroimagers (M.B. and A.G.) to exclude images with artifacts. To avoid errors during the brain extraction procedure, large nonbrain sections (i.e., neck) were removed by using the standard_space_roi tool, part of FSL (FMRIB Software Library, www.fmrib.ox.ac.uk/fsl/ (Jenkinson et al., 2012)). Bias field correction on T1-W images was performed with the nonparametric nonuniform intensity normalization (N4) algorithm (Nakamura et al., 2013), part of ANTs v2.10 (Advanced Normalization Tools, http://stnava.github.io/ANTs/) (Tustison et al., 2010). Images that failed the intensity inhomogeneity correction were excluded from analysis.

2.3.2. SIENA analysis

Global brain volume changes over time were quantified using the SIENA method (Smith et al., 2002), also part of FSL (version 5.0.10). This registration-based method uses images from two time points to assess BV changes by directly estimating the local shifts in brain edges across the entire brain and then converting the edge displacement into a global estimate of PBVC between the two time points. While using SIENA, a procedure of brain extraction able to improve the removal of nonbrain tissues was implemented for a more accurate BV estimation. The aim was to ensure that a consistent segmentation across time points of the intracranial region, which is the starting point of the SIENA analysis, was considered in the analysis of multiple MRI scans. Thus, we obtained within-subject brain mask as follows:

(1) Because previous studies (Cover et al., 2014; Popescu et al., 2012) showed that the performance of the FSL brain extraction tool (Smith, 2002) largely improves when using the bias field correction option "-B" with small values (i.e., 0.1 or 0.2) of the fractional intensity threshold option "-f", for each time-point image of the participant, five different brain masks were obtained by using the "-B" option and five different values of the "-f" option (from 0.05 to 0.25, increasing by 0.05). Among those masks, the one ensuring the best separation of brain from nonbrain tissue was selected, based on visual inspection, and its options were used for each participant's timepoint.
(2) The brain masks for each participant were aligned in the participant space, by using the results of the Anatomical-Average tool in FSL, which was run using the T1-weighted images.
(3) A single preliminary subject-brain mask was created by merging all the aligned time-point masks of that participant and retaining voxels that were segmented as the brain in more than 50% of the masks.
(4) If necessary, as final refinement, a manual editing of the preliminary subject-brain mask was performed and thus the within-subject brain mask was obtained.

Table 2
Intrasubject variability as assessed in participants with follow-up < 1 month

Center	No. of participants with follow-up <1 mo	No. of excluded participants	Causes of exclusion	Intrasubject variability
ADNI	96	1	Partial brain coverage	0.22% (0.001–1.78)
Amsterdam	1	0		0.65%
Boston	8	0		0.37% (0.04–0.72)
Graz	68	0		0.19% (0.003–1.23)
London	51	8	Poor GM/CSF contrast	0.37% (0.003–1.23)
Milan	131	3	Motion artifacts	0.22% (0.009–0.92)
Naples	6	0		0.1% (0.02–0.28)
Oxford	15	0		0.08% (0.001–0.24)
Prague	3	0		0.1% (0.02–0.16)
Rome	13	0		0.19% (0.01–1)
Siena	0	0		
Total	392	12 (3.07%)		0.25% (0.0001–1.78)

Number of participants excluded after quality control and the causes of exclusion are also reported. Intrasubject variability estimations are expressed as mean (range).
Key: ADNI, Alzheimer's Disease Neuroimaging Initiative; CSF, cerebrospinal fluid; GM, gray matter.

Table 3
Normative data as assessed in healthy individuals with follow-up > 6 months

Center	No. of participants with follow-up >6 mo	No. of excluded participants	Causes of exclusion
ADNI	78	2	Poor repositioning
Amsterdam	54	2	Motion artifacts
Boston	32	2	Poor repositioning Motion artifacts
Graz	14	5	Motion artifacts Poor repositioning
London	57	18	Poor GM/CSF contrast
Milan	28	0	
Naples	26	2	Motion artifacts
Oxford	15	3	Motion artifacts Field inhomogeneities
Prague	80	3	Motion artifacts Partial brain coverage
Rome	0	0	
Siena	37	0	
Total	421	37 (8.79%)	

Number of participants excluded after quality control and the causes of exclusion are also reported.
Key: ADNI, Alzheimer's Disease Neuroimaging Initiative; CSF, cerebrospinal fluid; GM, gray matter.

(5) Finally, the within-subject mask was transformed separately using trilinear interpolation into the 3D T1-W space of each time point and subsequently used to perform the final brain extraction.

Then, SIENA was run on each pair of images and data outputs were visually checked by expert neuroimagers (M.B. and A.G.) for a final quality assessment.

2.5. Statistical analysis

2.5.1. Intrasubject variability
Out of the whole data set of 720 healthy individuals, a subset of 392 participants with a follow-up <1 month was selected to assess the intrasubject variability of the BV measurement using the SIENA software in different acquisition settings. Given the interval between the scans in each participant, the intrasubject variability can be considered to include both physiological fluctuations of BV and the measurement error. The intrasubject variability was quantified as the absolute error of PBVC.

Generalized mixed linear models using the PBVC between two scans as dependent variable, magnetic field strength, vendor, and their interaction as fixed factors, and adding center as random variable were performed to explore the PBVC intrasubject variability in different acquisition settings. The analysis was run using the R software (https://www.r-project.org/).

2.5.2. Normative data
Out of the 720 healthy individuals, a subset of 421 participants with a follow-up > 6 months was used to obtain the normative values for PBVC/y. An arctangent (atan) transform was used to make the variance of PBVC/y independent of its mean value. Thus, analysis was performed by using the atan(PBVC/y) as dependent variable.

To select the variables independently associated to PBVC/y, stepwise mixed models with random intercept were run, using midpoint age between the two scans as covariate and sex, magnetic field strength, presence of distortion correction, and vendor as fixed factors. The final model included all the factors significantly ($p < 0.05$) associated to PBVC/y at multivariate analysis. The standard deviation of the residuals was used to create the normative range.

The mixed-effects model with participant as random effects is known to deal with the presence of multiple scan pairs for a given participant taking into account also the autocorrelation structure of

measures repeated over time on the same participant. This modeling approach allows obtaining (1) the components of the variance of PBVC/y as the intersubject variance ($\sigma^2_{Inter\ subj}$), which is linearly dependent on the length of follow-up, and (2) the intrasubject variance ($\sigma^2_{Intra\ subj}$), which is the variation due to the sum of the volume changes related to random physiological conditions at the scan time and the error of the software, and that is independent on the length of follow-up. Thus, naming fu the length of follow-up, $\sigma^2_{Inter\ subj-1y}$ the intersubject variance at 1 year of follow-up and $\sigma^2_{Intra\ subj}$ the fixed intrasubject variance, the total variance estimated by the final mixed model is the sum of these variance components according to the following formula:

$$sd_{fu} = \sqrt{\sigma^2_{Inter\ subj-1y} + \frac{(\sigma^2_{Intra\ subj})}{fu^2}} \quad (1)$$

The normative percentiles of PBVC/y were calculated using the formula:

$$CI^{year}_{fu} = \tan(Y^{fu}_{predicted} \pm XX * sd_{fu})$$

where $Y^{fu}_{predicted}$ is the PBVC/y as obtained by the regression model, XX was 0.84 for the 80th and 1.64 for the 95th percentile, respectively, as obtained by the one-sided Z distribution. Data were converted to the original scale by applying the inverse of the arctangent transform.

3. Results

3.1. Intrasubject variability of SIENA measurements

Data used for assessing the intrasubject variability are summarized in Table 2. Out of the 392 healthy individuals with MRI data sets of <1 month follow-up, 12 (3.07%) were excluded after quality control and a total of 536 SIENA analyses were run, as a number of participants had more than 1 pair of MRI scans.

The mean of the intrasubject variability, defined as the absolute error of PBVC, which includes the measurement error and short-term biological fluctuations (Opfer et al., 2018), was 0.25% (Table 2). Small and nonsignificant differences in intrasubject variability were found between scans acquired at 1.5 T and those acquired at 3T (mean: 0.22% at 1.5 T, 0.25% at 3T); data acquired with Philips scanners had slightly higher intrasubject variability than those acquired with Siemens and GE (mean: 0.28% for Philips, 0.17% for Siemens, 0.23% for GE).

3.2. Prediction of PBVC/y

Data used for assessing the normative BV rates are summarized in Table 3. Out of the 421 healthy individuals with follow-up MRI >6 months, 37 (8.78%) were excluded after quality control and a total of 789 SIENA analyses were run (Fig. 1), as a number of participants had more than 1 pair of MRI scans. The age of the group ranged from 16 to 90 years (mean ± SD: 45.7 ± 18.4 years) and 53.6% were female.

The model with the best fit for atan(PBVC/y), as assessed by the stepwise mixed model analysis, selected age and magnetic field strength as independent significant predictors ($R^2 = 0.18$; $p < 0.001$). The other factors such as sex, scanner vendor, and presence of distortion correction were discarded by the model.

3.2.1. Effect of magnetic field strength
PBVC/y measured on 3T scanners showed significantly smaller atrophy rate (0.127%, $p < 0.001$) than those on 1.5 T.
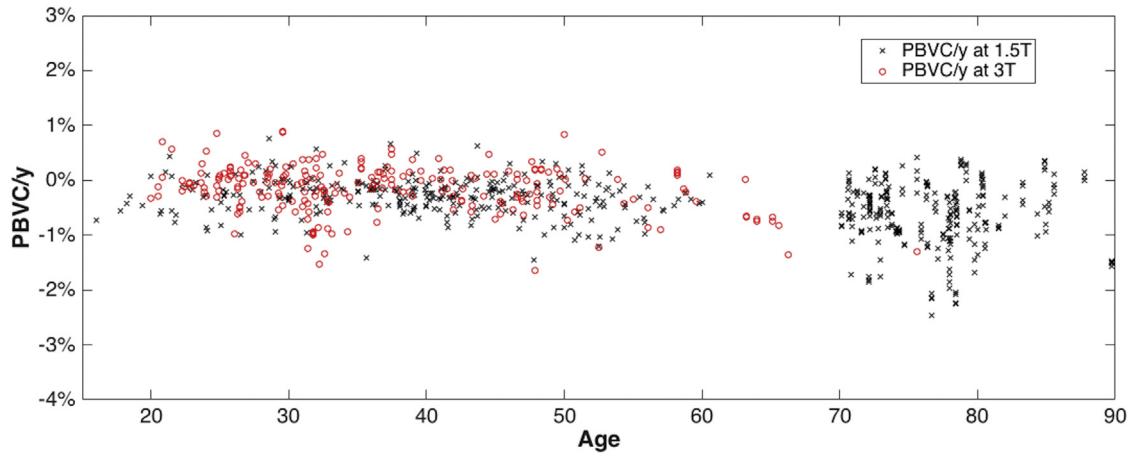
Fig. 1. Scatterplot of PBVC/y (Y-axis) against age (X-axis) of the 789 pairs of MRI images analyzed with SIENA. Abbreviations: MRI, magnetic resonance imaging; PBVC/y, yearly percentage brain volume change; SIENA, Structural Imaging Evaluation, using Normalization, of Atrophy.

3.2.2. Effect of age

The mean PBVC/y showed age-related increase over the adult lifespan. PBVC/y per age period and magnetic field strength are reported in Table 4 and Table 5, ranging from −0.13% at 1.5 T and −0.02% at 3T at the age of 20 years to −0.54% at 1.5 T and −0.4% at 3T at the age of 80 years.

3.2.3. Normative percentiles

The intrasubject variability estimated by the mixed model showed a standard deviation of 0.29%, which was close to the value estimated by using the scan pairs with follow-up <1 month. The intersubject variability of PBVC/y was estimated as a standard deviation of 0.16%.

As expected, the normative percentiles of PBVC/y showed an age-related increase over the adult lifespan. There were also significant differences when normative percentiles of PBVC/y were measured at 1.5T or 3T (Fig. 2). Furthermore, because the contribution of the intrasubject variability to the whole variance is divided by the follow-up length (see Equation 1), the variability of PBVC/y was narrower as the interscan interval was longer. For example, at 1.5 T, the 80th normative percentile of PBVC/y ranged from −0.48% at the age of 20 years to −0.92% at the age of 80 years when the PBVC was estimated over 1 year (see Table 4). Over 2-year follow-up, the 80th normative percentiles of PBVC/y values at 1.5 T ranged from −0.37% at the age of 20 years to −0.76% at the age of 80 years. In the same conditions, at 3T the 80th normative

percentiles of PBVC/y was −0.34% at the age of 20 years and −0.73% at the age of 80 years for 1-year follow-up, and −0.24% at the age of 20 years and −0.59% at the age of 80 years for 2-year follow-up (Table 5).

On the MAGNIMS web site (www.magnims.eu), a calculator will be made available to automatically calculate the expected PBVC/y for a given individual according to the relevant variables such as age, magnetic field strength, and interscan interval as inputs.

4. Discussion

The present work provides normative values of annualized total BV change (i.e., PBVC/y) as assessed by SIENA, an open-source software that is widely used for the assessment of BV changes on clinical MR scans (Guevara et al., 2017; Mak et al., 2015; Sastre-Garriga et al., 2015). Great effort has been devoted in pooling MRI data from a relatively large population of healthy individuals that were acquired from 34 different scanners with 11 different acquisition protocols. Thus, the study population should be representative of the whole adulthood (with age ranging from 16 to 90 years) and covers most of the real-world acquisition protocols, with MRI examinations performed with the 3 most used MR scanner vendors (i.e., General Electrics, Philips, Siemens) and clinical magnetic field strengths (i.e., 1.5 T and 3T). Interestingly, results clearly showed that, among all parameters, age and magnetic field strength were the significant predictors of PBVC/y.

Table 4
Predicted rate of PBVC/y at 1.5 T for different age ranges

Age range (y)	1.5 T			
	Predicted PBVC/y	Follow-up length	80th NP	95th NP
20–30	−0.17	1 y	−0.48	−0.87
		2 y	−0.37	−0.58
30–40	−0.23	1 y	−0.55	−0.98
		2 y	−0.44	−0.67
40–50	−0.29	1 y	−0.64	−1.10
		2 y	−0.51	−0.76
50–60	−0.36	1 y	−0.72	−1.24
		2 y	−0.59	−0.86
60–70	−0.43	1 y	−0.82	−1.41
		2 y	−0.67	−0.96
70–80	−0.50	1 y	−0.92	−1.60
		2 y	−0.76	−1.09

The 80th and 95th normative percentiles (NPs) for 1 and 2 y of follow-up are provided (see text for details).
Key: PBVC/y, yearly percentage brain volume change.

Table 5
Predicted rate of PBVC/y at 3T for different age ranges

Age range (y)	3T			
	Predicted PBVC/y	Follow-up length	80th NP	95th NP
20–30	−0.05	1 y	−0.34	−0.68
		2 y	−0.24	−0.44
30–40	−0.11	1 y	−0.41	−0.77
		2 y	−0.30	−0.51
40–50	−0.17	1 y	−0.48	−0.87
		2 y	−0.37	−0.59
50–60	−0.23	1 y	−0.56	−0.99
		2 y	−0.44	−0.67
60–70	−0.30	1 y	−0.64	−1.11
		2 y	−0.51	−0.76
70–80	−0.36	1 y	−0.73	−1.25
		2 y	−0.59	−0.86

The 80th and 95th normative percentiles (NPs) for 1 and 2 years of follow-up are provided (see text for details).
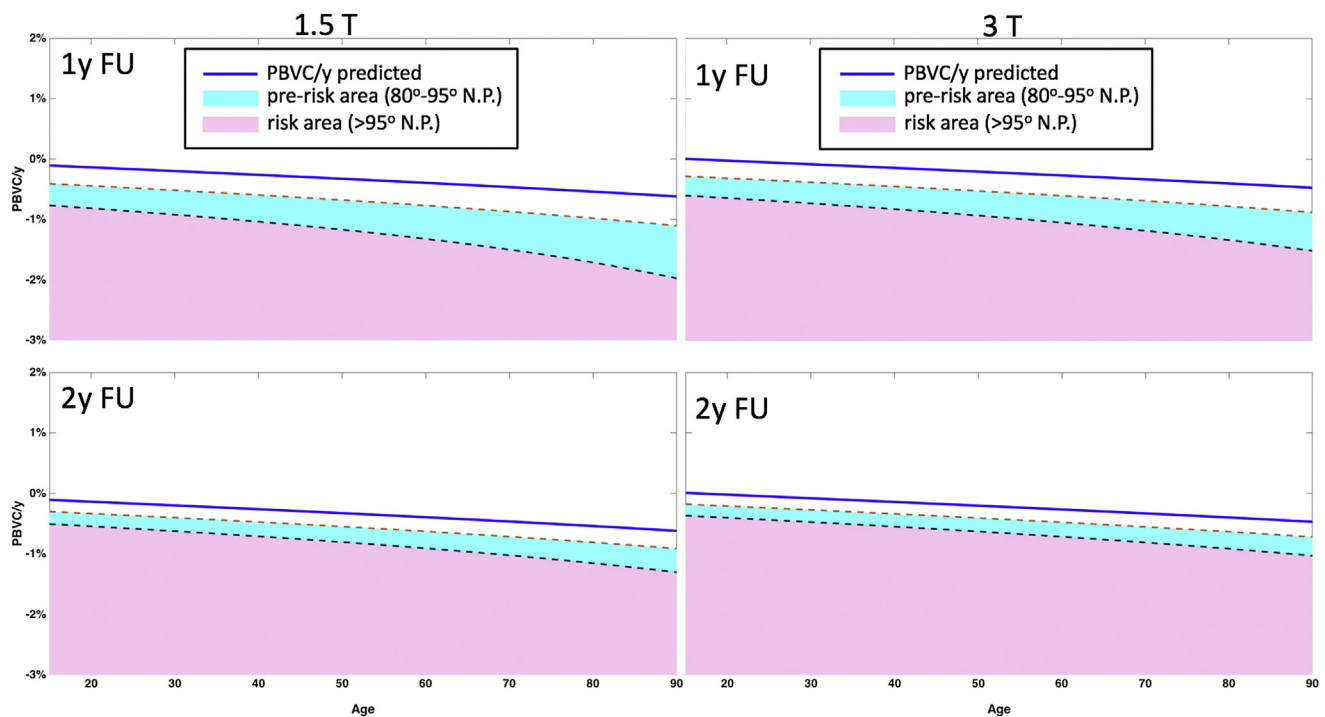Key: PBVC/y, yearly percentage brain volume change.

Fig. 2. Normative values of PBVC/y as obtained with SIENA at 1.5T (left side) and 3T (right side) for 1-year (top) and 2-year (bottom) follow-up. Predicted values as resulted from the model are shown in each panel (blue line). Also note, in each panel the values of PBVC/y which are within the 80th and 95th normative percentiles (NP, light blue areas) and higher than the 95th NP (pink areas) are represented. Abbreviations: PBVC/y, yearly percentage brain volume change; SIENA, Structural Imaging Evaluation, using Normalization, of Atrophy. (For interpretation of the references to color in this figure legend, the reader is referred to the Web version of this article.)

Data analysis showed an acceleration of BV loss during aging, with values of PBVC/y that doubled in individuals aged 60—70 years in comparison to those aged 30—40 years, independently of the MRI setting. This finding is expected (Liu et al., 2003; Takao et al., 2012) and was hypothesized as due to different temporal patterns of gray matter (GM) and white matter volume change, with the former linearly decreasing after adolescence and the latter being stable or slightly increasing until 45 years and decreasing thereafter (Hedman et al., 2012). This hypothesis could not be tested here because SIENA does not allow separate longitudinal analyses of GM and white matter volume changes. However, we plan to pursue this goal in the near future by using some of the recently proposed methods (Ashburner and Ridgway, 2013; Battaglini et al., 2018; Reuter and Fischl, 2011). In general, however, it is worth stressing that the increased range of normality with aging might also reflect a larger variability in the rate of BV change in older adults (Enzinger et al., 2005). Previous studies (De Stefano et al., 2017) have shown that presence/absence of specific habits (i.e., smoking, alcohol consumption, etc.) and/or comorbidities (i.e., hypertension, diabetes, obesity, etc.) have an impact on the rate of BV change, particularly with increasing age, and this might have had a significant role in the increased variability (i.e., increased PBVC/y) observed in our older participants (Resnick et al., 2003). Unfortunately, the retrospective design of the study did not allow the retrieval of this information.

As mentioned before, the multicenter data analyzed in the present study were acquired with different protocols (n = 11) on a relatively large number of MR scanners (n = 34) by the three most popular vendors and with the two magnetic field strengths currently used in the clinic setting (i.e., 1.5 T and 3T). Interestingly, our results showed that different MR protocols and scanner types did not add significant prediction to the rate of BV changes. However, our findings showed difference in BV rates on data acquired on scanners with different magnetic field strengths. This held true also in subgroup analyses of participants grouped for age, with the exclusion of those >65 years of age as they did not have scan acquisition at 3T (see Fig 1, data not shown). Because the two cohorts (1.5 T and 3T) included different individuals and differences could therefore be caused by cohort effects, we increased confidence in this finding by performing a post-hoc analysis on 41 healthy individuals from the ADNI data set who had 1-year follow-up data acquired at both 1.5 T and 3T. Lower BV changes were found on data acquired at 3T ($-0.51\% \pm 0.8$) with respect to those acquired at 1.5 T ($-0.68\% \pm 0.9$, $p = 0.04$, data not shown). Because 3 T images may have a better contrast at the GM/cerebrospinal fluid interface than 1.5 T images (Chu et al., 2016, 2017; Kruggel et al., 2010), this could have a great impact on the SIENA analysis, which is essentially based on the quantification of the shift at GM/cerebrospinal fluid interface between two time points. However, other causes such as different coil design (including parallel imaging), pulse sequence choice, k-space sampling schemes, and gradient strength might also explain the differences in BV changes between data acquired at 1.5 T and 3T, a finding that deserves further investigation.

When assessing MRI-derived BV changes in a population, the total variance comes from differences between individuals (intersubject variability) and from the random fluctuation of BV in each individual (intrasubject variability). Owing to the characteristics of our data set, we were able to measure here both types of variability. The intrasubject variability, which includes the measurement error and short-term biological fluctuations, in our study was very close to the within-patient fluctuations recently described by Opfer and coworkers (Opfer et al., 2018). In addition, in line with recent studies (Biberacher et al., 2016; Opfer et al., 2018), we found here a decreased intrasubject variability with longer follow-up (i.e., 2 years vs. 1 year). This has practical implications as, in providing normative percentiles of PBVC/y, the cutoff values are definitely influenced by measurement errors and short-term biological

fluctuations, so that the interval between the expected value and the 95th normative percentiles of PBVC/y was 40% smaller if obtained from MRI examinations at 2-year than at 1-year follow-up. In our data set, for example, if the range of normality is defined as the positive difference between the expected value and the 95th normative percentiles of PBVC/y, this was 40% more accurate if obtained from MRI examinations at 2-year than at 1-year follow-up. This suggests the need for a "dynamic" approach when using pathological cutoff values in clinical practice, in which the rate of BV change for a single patient should be assessed using a model (e.g., a calculator) that incorporates the various important factors such as age, magnetic field strength, and follow-up time. It is worth stressing that the proposed normative data have a larger error than those proposed in previous studies (De Stefano et al., 2016; Opfer et al., 2017). The aforementioned relevance of the follow-up length as well as the use in the present study of a large, multi-center data set with multiple acquisition protocols and settings can represent plausible explanations for this apparent discrepancy.

Overall, results reported in the present study showed that MRI-derived rates of BV changes are dependent on age, magnetic field strength, and follow-up length. All these parameters will be therefore included in a freely available calculator (www.magnims.eu), which is meant to automatically provide the normative range of PBVC/y for a given individual and thus the potential deviation from healthy conditions. It should be stressed here that the calculator output should not be used per se, but needs to be contextualized with all other individual information by the referring doctor. Although this tool does not overcome all constraints hampering the use of BV loss assessments in clinical practice (De Stefano et al., 2017; Rocca et al., 2017; Sastre-Garriga et al., 2017) and could certainly be improved in the future by adding further data and more refined assessments, it presently includes carefully assessed normative data of the rate of BV change that are representative of the whole adult lifespan and were acquired with the most frequent settings used in clinic. This should represent an easy-to-use tool that should facilitate the use and interpretation of brain atrophy in both research and clinical settings.

Disclosure

Acknowledgements

Appendix A. Supplementary data

Supplementary data to this article can be found online at https://doi.org/10.1016/j.neurobiolaging.2019.05.010.

References

Ashburner, J., Ridgway, G.R., 2013. Symmetric diffeomorphic modeling of longitudinal structural MRI. Front Neurosci. 6, 197.

Battaglini, M., Jenkinson, M., De Stefano, N., 2018. SIENA-XL for improving the assessment of gray and white matter volume changes on brain MRI. Hum. Brain Mapp. 39 (3), 1063—1077.

Biberacher, V., Schmidt, P., Keshavan, A., Boucard, C.C., Righart, R., Samann, P., Preibisch, C., Fröbel, D., Aly, L., Hemmer, B., Zimmer, C., Henry, R.G., Mühlau, M., 2016. Intra- and interscanner variability of magnetic resonance imaging based volumetry in multiple sclerosis. NeuroImage 142, 188—197.

Chu, R., Hurwitz, S., Tauhid, S., Bakshi, R., 2017. Automated segmentation of cerebral deep gray matter from MRI scans: effect of field strength on sensitivity and reliability. BMC Neurol. 17, 172.

Chu, R., Tauhid, S., Glanz, B.I., Healy, B.C., Kim, G., Oommen, V.V., Khalid, F., Neema, M., Bakshi, R., 2016. Whole brain volume measured from 1.5T versus 3T MRI in healthy participants and patients with multiple sclerosis. J. Neuroimaging 26, 62–67.

Cover, K.S., van Schijndel, R.A., Popescu, V., van Dijk, B.W., Redolfi, A., Knol, D.L., Frisoni, G.B., Barkhof, F., Vrenken, H., neuGRID, Alzheimer's Disease Neuroimaging Initiative, 2014. The SIENA/FSL whole brain atrophy algorithm is no more reproducible at 3T than 1.5 T for Alzheimer's disease. Psychiatry Res. 224, 14–21.

De Stefano, N., Airas, L., Grigoriadis, N., Mattle, H.P., O'Riordan, J., Oreja-Guevara, C., Sellebjerg, F., Stankoff, B., Walczak, A., Wiendl, H., Kieseier, B.C., 2014. Clinical relevance of brain volume measures in multiple sclerosis. CNS Drugs 28, 147–156.

De Stefano, N., Silva, D.G., Barnett, M.H., 2017. Effect of fingolimod on brain volume loss in patients with multiple sclerosis. CNS Drugs 31, 289–305.

De Stefano, N., Stromillo, M.L., Giorgio, A., Bartolozzi, M.L., Battaglini, M., Baldini, M., Portaccio, E., Amato, M.P., Sormani, M.P., 2016. Establishing pathological cut-offs of brain atrophy rates in multiple sclerosis. J. Neurol. Neurosurg. Psychiatry 87, 93–99.

Driscoll, I., Davatzikos, C., An, Y., Wu, X., Shen, D., Kraut, M., Resnick, S.M., 2009. Longitudinal pattern of regional brain volume change differentiates normal aging from MCI. Neurology 72, 1906–1913.

Enzinger, C., Fazekas, F., Matthews, P.M., Ropele, S., Schmidt, H., Smith, S., Schmidt, R., 2005. Risk factors for progression of brain atrophy in aging: six-year follow-up of normal participants. Neurology 64, 1704–1711.

Fotenos, A.F., Snyder, A.Z., Girton, L.E., Morris, J.C., Buckner, R.L., 2005. Normative estimates of cross-sectional and longitudinal brain volume decline in aging and AD. Neurology 64, 1032–1039.

Frisoni, G.B., Fox, N.C., Jack Jr., C.R., Scheltens, P., Thompson, P.M., 2010. The clinical use of structural MRI in Alzheimer disease. Nat. Rev. Neurol. 6, 67–77.

Giorgio, A., De Stefano, N., 2013. Clinical use of brain volumetry. J. Magn. Reson. Imaging 37, 1–14.

Guevara, C., Bulatova, K., Soruco, W., Gonzalez, G., Farias, G.A., 2017. Retrospective diagnosis of Parkinsonian syndromes using whole-brain atrophy rates. Front Aging Neurosci. 9, 99.

Hedman, A.M., van Haren, N.E., Schnack, H.G., Kahn, R.S., Hulshoff Pol, H.E., 2012. Human brain changes across the life span: a review of 56 longitudinal magnetic resonance imaging studies. Hum. Brain Mapp. 33, 1987–2002.

Hotter, A., Esterhammer, R., Schocke, M.F., Seppi, K., 2009. Potential of advanced MR imaging techniques in the differential diagnosis of parkinsonism. Mov. Disord. 24 (Suppl 2), S711–S720.

Jenkinson, M., Beckmann, C.F., Behrens, T.E., Woolrich, M.W., Smith, S.M., 2012. FSL. Neuroimage. 62, 782–790.

Kruggel, F., Turner, J., Muftuler, L.T., 2010. Impact of scanner hardware and imaging protocol on image quality and compartment volume precision in the ADNI cohort. NeuroImage 49, 2123–2133.

Liu, R.S., Lemieux, L., Bell, G.S., Sisodiya, S.M., Shorvon, S.D., Sander, J.W., Duncan, J.S., 2003. A longitudinal study of brain morphometrics using quantitative magnetic resonance imaging and difference image analysis. NeuroImage 20, 22–33.

Mak, E., Su, L., Williams, G.B., Watson, R., Firbank, M., Blamire, A.M., O'Brien, J.T., 2015. Longitudinal assessment of global and regional atrophy rates in Alzheimer's disease and dementia with Lewy bodies. Neuroimage Clin. 7, 456–462.

Marcus, D.S., Fotenos, A.F., Csernansky, J.G., Morris, J.C., Buckner, R.L., 2010. Open access series of imaging studies: longitudinal MRI data in nondemented and demented older adults. J. Cogn. Neurosci. 22, 2677–2684.

Nakamura, K., Guizard, N., Fonov, V.S., Narayanan, S., Collins, D.L., Arnold, D.L., 2013. Jacobian integration method increases the statistical power to measure gray matter atrophy in multiple sclerosis. Neuroimage Clin. 4, 10–17.

Opfer, R., Ostwaldt, A.C., Sormani, M.P., Gocke, C., Walker-Egger, C., Manogaran, P., De Stefano, N., Schippling, S., 2017. Estimates of age-dependent cutoffs for pathological brain volume loss using SIENA/FSL-a longitudinal brain volumetry study in healthy adults. Neurobiol. Aging 65, 1–6.

Opfer, R., Ostwaldt, A.C., Walker-Egger, C., Manogaran, P., Sormani, M.P., De Stefano, N., Schippling, S., 2018. Within-patient fluctuation of brain volume estimates from short-term repeated MRI measurements using SIENA/FSL. J. Neurol. 265, 1158–1165.

Popescu, V., Battaglini, M., Hoogstrate, W.S., Verfaillie, S.C., Sluimer, I.C., van Schijndel, R.A., van Dijk, B.W., Cover, K.S., Knol, D.L., Jenkinson, M., Barkhof, F., de Stefano, N., Vrenken, H., MAGNIMS Study Group, 2012. Optimizing parameter choice for FSL-Brain Extraction Tool (BET) on 3D T1 images in multiple sclerosis. NeuroImage 61, 1484–1494.

Resnick, S.M., Pham, D.L., Kraut, M.A., Zonderman, A.B., Davatzikos, C., 2003. Longitudinal magnetic resonance imaging studies of older adults: a shrinking brain. J. Neurosci. 23, 3295–3301.

Reuter, M., Fischl, B., 2011. Avoiding asymmetry-induced bias in longitudinal image processing. NeuroImage 57, 19–21.

Rocca, M.A., Battaglini, M., Benedict, R.H., De Stefano, N., Geurts, J.J., Henry, R.G., Horsfield, M.A., Jenkinson, M., Pagani, E., Filippi, M., 2017. Brain MRI atrophy quantification in MS: from methods to clinical application. Neurology 88, 403–413.

Sastre-Garriga, J., Pareto, D., Rovira, A., 2017. Brain atrophy in multiple sclerosis: clinical relevance and technical aspects. Neuroimaging Clin. N. Am. 27, 289–300.

Sastre-Garriga, J., Tur, C., Pareto, D., Vidal-Jordana, A., Auger, C., Rio, J., Huerga, E., Tintoré, M., Rovira, A., Montalban, X., 2015. Brain atrophy in natalizumab-treated patients: a 3-year follow-up. Mult. Scler. (Houndmills, Basingstoke, England) 21, 749–756.

Smith, S.M., 2002. Fast robust automated brain extraction. Hum. Brain Mapp. 17 (3), 143–155.

Smith, S.M., Zhang, Y., Jenkinson, M., Chen, J., Matthews, P.M., Federico, A., De Stefano, N., 2002. Accurate, robust, and automated longitudinal and cross-sectional brain change analysis. NeuroImage 17, 479–489.

Takao, H., Hayashi, N., Ohtomo, K., 2012. A longitudinal study of brain volume changes in normal aging. Eur. J. Radiol. 81, 2801–2804.

Tustison, N.J., Avants, B.B., Cook, P.A., Zheng, Y., Egan, A., Yushkevich, P.A., Gee, J.C., 2010. N4ITK: improved N3 bias correction. IEEE Trans. Med. Imaging 29, 1310–1320.

van Maurik, I.S., Zwan, M.D., Tijms, B.M., Bouwman, F.H., Teunissen, C.E., Scheltens, P., Wattjes, M.P., Barkhof, F., Berkhof, J., van der Flier, W.M.1., Alzheimer's Disease Neuroimaging Initiative, 2017. Interpreting biomarker results in individual patients with mild cognitive impairment in the Alzheimer's biomarkers in daily practice (ABIDE) project. JAMA Neurol. 74, 1481–1491.

Vrenken, H., Jenkinson, M., Horsfield, M.A., Battaglini, M., van Schijndel, R.A., Rostrup, E., Geurts, J.J., Fisher, E., Zijdenbos, A., Ashburner, J., Miller, D.H., Filippi, M., Fazekas, F., Rovaris, M., Rovira, A., Barkhof, F., de Stefano, N., MAGNIMS Study Group, 2013. Recommendations to improve imaging and analysis of brain lesion load and atrophy in longitudinal studies of multiple sclerosis. J. Neurol. 260, 2458–2471.